Chemiresistors for Array-Based Vapor Sensing Using Composites of Carbon Black with Low Volatility Organic Molecules

Ting Gao, Marc D. Woodka, Bruce S. Brunschwig, and Nathan S. Lewis*

210 Noyes Laboratory, 127-72, Division of Chemistry and Chemical Engineering, California Institute of Technology, Pasadena, California 91125

Received April 19, 2006. Revised Manuscript Received June 20, 2006

Chemically sensitive resistors have been fabricated from composites of carbon black and low volatility, nonpolymeric, organic molecules such as propyl gallate, lauric acid, and dioctyl phthalate. Sorption of organic vapors into the nonconductive phase of such composites produced rapid and reversible changes in the relative differential resistance response of the sensing films. Arrays of these sensors, in which each sensing film was comprised of carbon black and a chemically distinct nonpolymeric organic molecule or blend of organic molecules, produced characteristic response patterns upon exposure to a series of different organic test vapors. The use of nonpolymeric sorption phases allowed fabrication of sensors having a high density of randomly oriented functional groups and provided excellent discrimination between analytes. By comparison to carbon black−polymer composite vapor sensors and sensor arrays, such sensors provided comparable detection limits as well as enhanced clustering and enhanced resolution ability between test analytes.

I. Introduction

Array-based vapor sensing has attracted significant interest for its ability to detect and discriminate between various analyte vapors.[1] Surface acoustic wave devices,[2−4] tin oxide sensors,[5−7] conducting organic polymers,[8−10] polymer-coated quartz crystal microbalances,[11−13] polymer-coated micromachined cantilevers,[14] thin film capacitors,[15] dye-impregnated polymers coated onto optical fibers or beads,[16−18] transition metal-based dyes,[19,20] and polymer composite chemically sensitive resistors[21−23] have all been explored in array-based sensing approaches. In this architecture, each sensor is not designed to respond selectively to a single analyte, but instead each analyte produces a distinct fingerprint from the array of broadly cross-reactive sensors. Pattern recognition algorithms can then be used to obtain information on the identity, properties, and concentration of the vapor exposed to the sensor array.[24−27]

One especially attractive signal transduction mode involves the use of chemically sensitive resistors as the sensor array elements.[21−23] Such sensors are inherently low power,[28,29] are compatible with very large-scale integration (VLSI) processing,[7,30] can be deposited onto a variety of substrates including interdigitated electrodes,[31] glass,[32] ceramic,[33] or

* To whom correspondence should be addressed. Phone: 626-395-6335. Fax: 626-395-8867. E-mail: nslewis@its.caltech.edu. Home Page: http://nsl.caltech.edu.

(1) Albert, K. J.; Lewis, N. S.; Schauer, C. L.; Sotzing, G. A.; Stitzel, S. E.; Vaid, T. P.; Walt, D. R. *Chem. Rev.* **2000**, *100*, 2595.
(2) Ballantine, D. S.; Rose, S. L.; Grate, J. W.; Wohltjen, H. *Anal. Chem.* **1986**, *58*, 3058.
(3) Rose-Pehrsson, S.; Grate, J.; Ballantine, D. S.; Jurs, P. C. *Anal. Chem.* **1988**, *60*, 2801.
(4) Patrash, S. J.; Zellers, E. T. *Anal. Chem.* **1993**, *65*, 2055.
(5) Srivastava, R.; Dwivedi, R.; Srivastava, S. K. *Sens. Actuators, B* **1998**, *50*, 175.
(6) Getino, J.; Horrillo, M. C.; Gutierrez, J.; Ares, L.; Robla, J. I.; Garcia, C.; Sayago, I. *Sens. Actuators, B* **1997**, *43*, 200.
(7) Bednarczyk, D.; DeWeerth, S. P. *Sens. Actuators, B* **1995**, *27*, 271.
(8) Huang, J.; Virji, S.; Weiller, B. H.; Kaner, R. B. *Chem.—Eur. J.* **2004**, *10*, 1315.
(9) Partridge, A. C.; Jansen, M. L.; Arnold, W. M. *Mater. Sci.* **2000**, *12*, 37.
(10) Bartlett, P. N.; Archer, P. B. M.; Lingchung, S. K. *Sens. Actuators* **1989**, *19*, 125.
(11) Fu, Y.; Finklea, H. O. *Anal. Chem.* **2003**, *75*, 5387.
(12) Haupt, K.; Noworyta, K.; Kutner, W. *Anal. Commun.* **1999**, *36*, 391.
(13) Mirmohseni, A.; Oladegaragoze, A. *Sens. Actuators, B* **2004**, *102*, 261.
(14) Lang, H. P.; Baller, M. K.; Berger, R.; Gerber, C.; Gimzewski, J. K.; Battiston, F. M.; Fornaro, P.; Ramseyer, J. P.; Meyer, E.; Guntherodt, H. J. *Anal. Chim. Acta* **1999**, *393*, 59.
(15) Willing, B.; Kohli, M.; Muralt, P.; Oehler, O. *Infrared Phys. Technol.* **1998**, *39*, 443.
(16) Albert, K. J.; Walt, D. R.; Gill, D. S.; Pearce, T. C. *Anal. Chem.* **2001**, 2501.
(17) Dickinson, T. A.; White, J.; Kauer, J. S.; Walt, D. R. *Nature* **1996**, *382*, 697.
(18) Goodey, A.; Lavigne, J. J.; Savoy, S. M.; Rodriguez, M. D.; Curey, T.; Tsao, A.; Simmons, G.; Wright, J.; Yoo, S. J.; Sohn, Y.; Anslyn, E. V.; Shear, J. B.; Neikirk, D. P.; McDevitt, J. T. *J. Am. Chem. Soc.* **2001**, 2559.
(19) Daws, C. A.; Exstrom, C. L.; Sowa, J. R.; Mann, K. R. *Chem. Mater.* **1997**, 363.
(20) Rakow, N. A.; Suslick, K. S. *Nature* **2000**, *406*, 710.
(21) Burl, M. C.; Sisk, B. C.; Vaid, T. P.; Lewis, N. S. *Sens. Actuators, B* **2002**, *87*, 130.
(22) Freund, M. S.; Lewis, N. S. *Proc. Natl. Acad. Sci. U.S.A.* **1995**, *92*, 2652.
(23) Lonergan, M. C.; Severin, E. J.; Doleman, B. J.; Beaber, S. A.; Grubbs, R. H.; Lewis, N. S. *Chem. Mater.* **1996**, *8*, 2298.
(24) Geladi, P.; Kowalski, B. R. *Anal. Chim. Acta* **1986**, *185*, 1.
(25) Burns, J. A.; Whitesides, G. M. *Chem. Rev.* **1993**, *93*, 2583.
(26) Kowalski, B. R.; Bender, C. F. *Anal. Chem.* **1972**, *44*, 1405.
(27) Duda, R. O.; Hart, P. E. *Pattern Classification and Scene Analysis*; John Wiley & Sons: New York, 1973.
(28) Korotchenkov, G. S.; Dmitriev, S. V.; Brynzari, V. I. *Sens. Actuators, B* **1999**, *54*, 202.
(29) Han, K. R.; Kim, C. S.; Kang, K. T.; Koo, H. J.; Il Kang, D.; He, J. W. *Sens. Actuators, B* **2002**, *81*, 182.
(30) Wilson, D. M.; Deweerth, S. P. *Sens. Mater.* **1998**, *10*, 169.
(31) Shurmer, H. V.; Corcoran, P.; Gardner, J. W. *Sens. Actuators, B* **1991**, *4*, 29.
(32) Briglin, S. M.; Freund, M. S.; Tokumaru, P.; Lewis, N. S. *Sens. Actuators, B* **2002**, *82*, 54.
(33) Shurmer, H. V.; Gardner, J. W.; Corcoran, P. *Sens. Actuators, B* **1990**, *1*, 256.

10.1021/cm060905x CCC: $33.50
Published on Web 09/28/2006

Scheme 1. Structures of Materials Used in This Study[a]

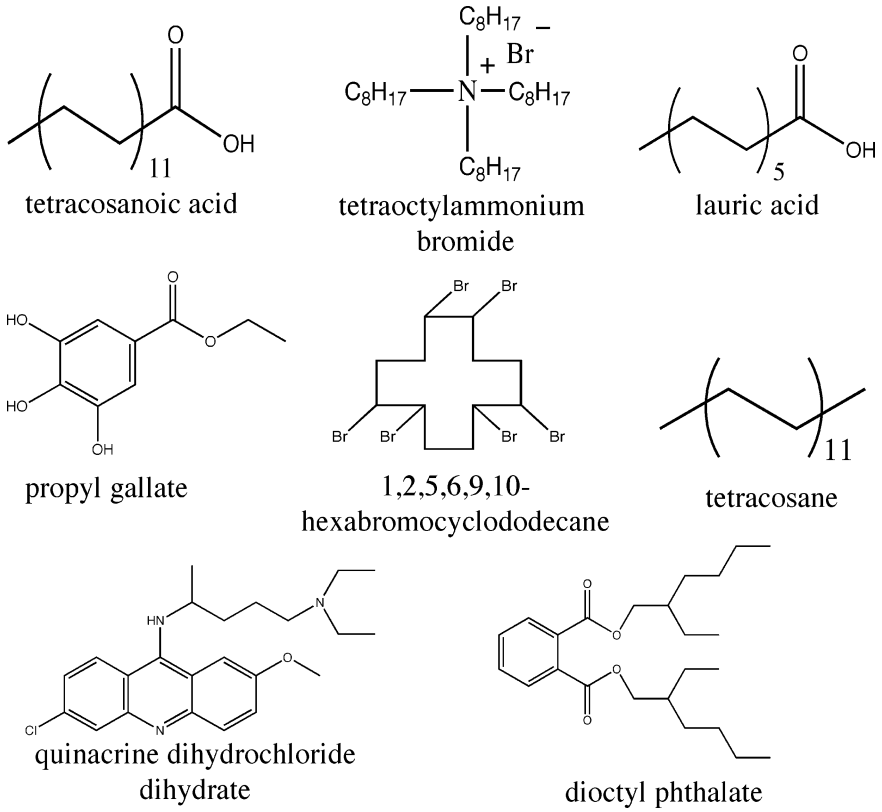

[a] All of these materials, except dioctyl phthalate, are solids at room temperature.

other insulating materials, and can be fabricated in a wide variety of form factors to optimize signal-to-noise ratios (SNRs) and produce desired physical sensor and sensor array configurations.[32] Significant attention in our laboratory has been devoted to the investigation of chemiresistive vapor detectors fabricated from composites of carbon black and insulating organic polymers,[21,22,32,34,35] in which the carbon black serves as the electrically conductive phase and the organic polymeric phase absorbs the organic vapor into the sensor.

The sensitivity of sorption-based detectors depends on the interactions between the analyte and the sorption material.[36] Vapor sensors with enhanced sensitivity to analytes having specific functional groups, such as amines or carboxylic acids, can be obtained through fabrication of sorption materials which target functional groups of the analyte of interest.[37,38] Increasing the density of the functional groups in the sorption material could further increase the amount of vapor sorption and therefore produce an additional increase in the sensitivity of such chemically resistive vapor detectors. In this work, we describe the properties of chemiresistive vapor sensors that are comprised of composites of conductive carbon black particles and an insulating organic material, wherein the sorption phase consists of simple, monomeric, low vapor pressure organic materials. Such sorption films have a relatively high density of functional groups and thereby could provide very effective sorption of organic analyte vapors. The random arrangement of the organic molecules in the sorption phase should produce a high vapor permeability and therefore lead to rapid sensor response times and could produce highly reversible responses that show relatively little history efforts or hysteresis in response to a wide range of organic analyte vapors. The use of nonpolymeric materials opens up a wide range of sorption phases having desirable chemical functionality and physical properties that are in general not readily accessible in polymeric materials.

II. Experimental Section

A. Materials. The insulating materials used in fabricating the sensor films (Scheme 1) and the plasticizer dioctyl phthalate were used as received from either Aldrich Chemical Co. or Acros Organics Co. Reagent grade toluene, *n*-hexane, tetrahydrofuran (THF), ethanol, ethyl acetate, cyclohexane, *n*-heptane, *n*-octane, and isooctane were used as received from Aldrich Chemical Co. Black Pearls 2000 (BP 2000), a furnace carbon black material, was donated by Cabot Co. (Billerica, MA) and was used as received.

B. Detectors. Detector substrates were fabricated by evaporating 300 nm of chromium and 700 nm of gold onto glass microscope slides using 0.2 cm wide drafting tape as a mask. After evaporation, the mask was removed and the glass slides were cut into 1.0 cm × 2.5 cm pieces.

Sensor films consisted of suspensions of various amounts of carbon black and either pure organic material or mixtures thereof

(34) Doleman, B. J.; Lonergan, M. C.; Severin, E. J.; Vaid, T. P.; Lewis, N. S. *Anal. Chem.* **1998**, *70*, 4177.
(35) Severin, E. J.; Doleman, B. J.; Lewis, N. S. *Anal. Chem.* **2000**, *72*, 658.
(36) Popovska-Pavlovska, F.; Raka, L. *J. Polym. Sci., Part B: Polym. Phys.* **2004**, *42*, 267.
(37) Tillman, E. S.; Koscho, M. E.; Grubbs, R. H.; Lewis, N. S. *Anal. Chem.* **2003**, *75*, 1748.
(38) Sotzing, G. A.; Phend, J. N.; Grubbs, R. H.; Lewis, N. S. *Chem. Mater.* **2000**, *12*, 593.

Table 1. Sorption Material Used in Carbon Black−Nonpolymeric Composite Sensors for (a) 75% and (b) 25% (by Mass) Carbon Black Loadings[a] and (c) Sorption Material Used in Carbon Black−Polymer Composite Sensors,[b] As Reported Previously[43]

		amount (mg)		
sensor	sorption material	sorption	plasticizer	CB
	(a) 75% Carbon Black Loading			
A1	propyl gallate	50	0	150
A2	quinacrine dihydrochloride dihydrate	50	0	150
A3	lauric acid/dioctyl phthalate	35	15	150
A4	tetracosane/dioctyl phthalate	35	15	150
A5	tetracosanoic acid	50	0	150
A6	quinacrine dihydrochloride dihydrate/dioctyl phthalate	35	15	150
A7	tetracosanoic acid/dioctyl phthalate	35	15	150
	(b) 20−25% Carbon Black Loading			
B1	tetraoctylammonium bromide/dioctyl phthalate	80	80	20
B2	lauric acid/dioctyl phthalate	80	70	20
B3	tetracosanoic acid	80	0	30
B4	tetracosanoic acid/dioctyl phthalate	80	50	20
B5	tetracosanoic acid/dioctyl phthalate	100	60	40
B6	propyl gallate	160	0	40
B7	1,2,5,6,9,10-hexabromocyclo-dodecane/dioctyl phthalate	100	60	40
B8	quinacrine dihydrochloride dihydrate	160	0	40
B9	quinacrine dihydrochloride dihydrate/dioctyl phthalate	100	60	40

(c) Previously Reported Sorption Materials

sensor	sorption material
C1	polycaprolactone (PCL)
C2	poly(ethylene-*co*-vinyl acetate) (PEVA)
C3	poly(ethylene oxide) (PEO)
C4	poly(ethylene glycol)
C5	poly(methyl vinyl ether-*co*-maleic anhydride)
C6	poly(4-vinyl phenol)
C7	polycarbonate
C8	poly(vinyl butyral)
C9	polystyrene (PVS)

[a] Plasticizer denotes the amount of dioctyl phthalate. A total of 20 mL of either THF or toluene was added to sorption and plasticizer materials, followed by addition of carbon black (CB) and by sonication for >30 min. [b] Fabricated with 40% of the stated sorption material, 40% di(ethylene glycol) dibenzoate (plasticizer), and 20% (by wt) of carbon black.

in 20 mL of either toluene or THF. Typically, the desired mass of organic sorption material was dissolved in 20 mL of solvent, and sufficient carbon black was then suspended in this solution to produce the desired mass fraction of organic material and carbon black, by weight of solids (Table 1). Prior to fabrication of the sensor films, the casting suspension was sonicated for >30 min at room temperature. An airbrush (Iwata, Inc.) was used[39] to spray these suspensions across the 0.2 cm gap on the detector substrates until the resistance between the two leads was 10−100 kΩ, as measured by a Keithley model 2002 multimeter. After fabrication, all sensors were placed in a stream of dry air for at least 24 h prior to exposure to the test analytes.

C. Measurements. The instrumentation and apparatus for resistance measurements and for delivery of analyte vapors has been described previously.[23,34,35] The array of sensors was housed in a stainless steel assembly that was connected by Teflon tubing to a computer-controlled, calibrated vapor generation and delivery system. To initiate an experiment, the detectors were placed into a flow chamber, and an air flow of 5 L min^{-1} containing 1.10 ± 0.15 parts per thousand (ppth) of water vapor was introduced until the resistance of the detectors stabilized. An individual analyte exposure to the detectors consisted of a three-step process that was initiated with 70 s of airflow to achieve a smooth baseline resistance. Analyte vapor at a controlled concentration in flowing air was then introduced to the detectors for 80 s, followed by 60 s of airflow to ensure that the baseline resistance value was restored before the next exposure.

Analytes consisted of five nonpolar hydrocarbons (cyclohexane, *n*-hexane, *n*-heptane, *n*-octane, and isooctane) as well as ethanol and ethyl acetate. In the primary set of data collection for composite sensors having high carbon black loadings, these seven analytes were presented in random order 200 times each to the detector array during a single run over 4 days, at a partial pressure in air such that $P/P^0 = 0.0050$, where P is the partial pressure and P^0 is the vapor pressure of the analyte at room temperature. In a separate run to evaluate the concentration dependence of the sensor response, concentrations of *n*-hexane and ethanol were varied at 10 different values of P/P^0 within the range $0.002 < P/P^0 < 0.07$, with five exposures to each analyte/concentration combination, in randomized order. Each exposure consisted of 100 s of laboratory air, followed by 100 s of analyte and by 100 s of laboratory air, at a flow rate of 5 L min^{-1}.

An identical data run was used to evaluate the performance of the sensors with low carbon black loadings, with the seven analytes presented in random order 200 times each to the detector array during a single run over 4 days. Additionally, subsequent runs which were identical in their randomized analyte exposure order, exposure times, and protocols were performed to assess the long-term drift and stability of the sensors. The second run was initiated 2 days after the completion of the first run; the third run was initiated 2 days after the completion of the second run, and the fourth run was initiated 6 months after the completion of the third run. In these experiments, analytes were presented to the detector array at concentrations corresponding to $P/P^0 = 0.0050$.

D. Data Processing. The response of a sensor to a particular analyte was expressed as $\Delta R_{max}/R_b$, where R_b is the baseline resistance of the sensor and ΔR_{max} is the steady-state resistance change upon exposing the sensor to analyte (after correcting for baseline drift). The value of ΔR_{max} was obtained from $R_{max} - R_b$, where R_{max} is the maximum resistance value observed during the analyte exposure, calculated by averaging over at least three consecutive resistance measurements (in most cases four or five) in the steady-state portion of the response signal. The value of R_b was calculated by averaging over five resistance measurements before the exposure was initiated. The ratiometric quantity $\Delta R_{max}/R_b$ was used as the response descriptor because it has been shown in similar detector films to be both relatively insensitive to the vapor introduction technique and to increase linearly with analyte concentration.[23,35] All data processing was performed using Matlab (The Mathworks, Natick, MA).

E. Quantification of Classification Performance. For quantification of the analyte classification performance, the responses from each of the data sets were sum-normalized. This process was performed using eq 1:

$$S'_{ij} = \frac{S_{ij}}{\sum_{j=1}^{n} S_{ij}} \quad (1)$$

where S_{ij} refers to the $\Delta R_{max}/R_b$ sensor response signal of the jth detector (out of n total detectors) to the ith analyte exposure, and S'_{ij} represents the sum-normalized analogue of S_{ij}. For sensors exhibiting a response that is linear with analyte concentration, this

(39) Koscho, M. E.; Grubbs, R. H.; Lewis, N. S. *Anal. Chem* **2002**, *74*, 1307.

normalization procedure produces a unit vector in *n*-dimensional space defining a location in this space characteristic of each test analyte, regardless of analyte concentration.

The Fisher linear discriminant (FLD) algorithm was used on sum-normalized sensor response data to analyze the classification performance of the sensors. In the FLD approach, the responses of a training set are used to calculate a vector that projects response data onto the one-dimensional space that maximizes the separation between two sets of data clusters.[40] For normalized data (eq 1) produced by the responses of an *n*-detector array, this projection has the form

$$D_i = \sum_{j=1}^{n-1} c_j S'_{ij} \tag{2}$$

where c_j represents one of the $n - 1$ weighting factors from the hyperplane determined by the FLD algorithm. The value of D_i (hereafter referred to as the D value) is a single, scalar metric that characterizes the position, along a vector normal to the hyperplane decision boundary, of the detector array data produced by an individual analyte exposure. The chosen hyperplane decision boundary is defined as the point in one-dimensional projected space for which a data point lying on this plane has an equal probability of belonging to either of the two data clusters.

The FLD algorithm maximizes the separation, or clustering, of the two distinct populations of D values that arise from a single binary separation task. This clustering is measured by the resolution factor (rf) characteristic of a separation task, as given in eq 3:[27]

$$\mathrm{rf} = \frac{\delta}{(\sigma_1^2 + \sigma_2^2)^{0.5}} \tag{3}$$

Here, δ is the difference in the population means of the D values, and σ_1 and σ_2 are the standard deviations of the two populations of D values that correspond to the two analytes of the separation task. The FLD algorithm was used to evaluate the separation between each possible pairwise combination of analytes in the data set.

Because a supervised algorithm inherently introduces some bias into the analysis, a train/test scheme was employed. For each pair of analytes that comprised a single separation task, the first 100 exposures to each analyte (exposures 1−100, data set 1) were used to generate a training set and a set of coefficients (comprising a classification model) as described in eq 2. A decision boundary was then developed by defining the hyperplane at which an unknown analyte exposure would have an equal probability (according to eq 3) of belonging to either analyte population of the given binary separation task. All subsequent data were treated as test data, in that the Fisher algorithm was not performed after the training phase, and analyte identities were classified according to their positions relative to the fixed FLD decision boundary.

The SNR of a sensor for a given exposure was calculated as

$$\mathrm{SNR} = \frac{\Delta R_{\max}}{\sigma_{\mathrm{baseline}}} \tag{4}$$

where $\sigma_{\mathrm{baseline}}$ represents the standard deviation in baseline resistance before analyte delivery, calculated using at least five data points.

The same analytes at $P/P^0 = 0.0050$ have been previously exposed to carbon black−polymer composite chemiresistors. Such data have been analyzed in the same manner as those for the sensors under study and are given for comparison.[21,22,32,34,35] Specifically, resolution factors and SNRs were compared for both types of sensors from previously recorded and reported data. For detection limit determination, carbon black−polymer composite sensors were also exposed simultaneously with carbon black−nonpolymer composite sensors to ensure equal vapor deliveries and representative analyses.

(40) Fisher, R. A. *Ann. Eugenic* **1936**, 179.

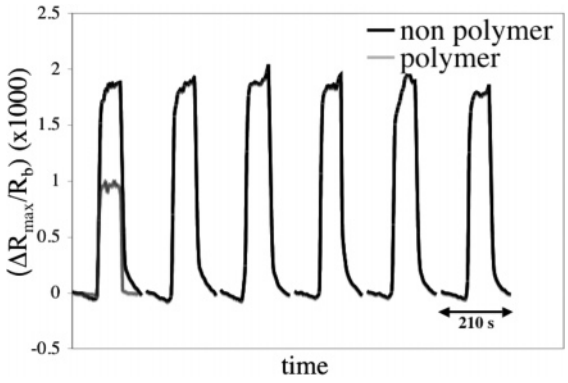

Figure 1. Response of a tetracosanoic acid/dioctyl phthalate (75% carbon black) composite (sensor A4) and a poly(ethylene-*co*-vinyl acetate) (40% carbon black) composite (sensor C2) on exposure to *n*-hexane at $P/P^0 = 0.0050$. Of all the sensors employed in this study, these two exhibited the highest signal and lowest noise upon exposure to *n*-hexane. Additionally, six exposures of the nonpolymer−carbon black composite sensor (A4) are shown. A total of 1, 35, 44, 62, and 71 h, as well as continuous random exposures to each of the test analytes, occurred between the first response shown and the second, third, fourth, fifth, and sixth responses.

III. Results

A. Vapor Response Characteristics and Reproducibility. Carbon black loadings of ≈10, 25, 50, and 75 wt % were investigated, and 75% loadings exhibited a higher SNR, lower detection limit, and enhanced clustering relative to other loadings. Thus, results on sensor films made from 75% carbon black loadings are primarily reported herein. Additional results are described for a 6-month stability and drift study that was performed on sensors having various lower carbon black loading levels. In each case, the carbon black loading was sufficient to ensure that the chemiresistors were above their percolation threshold, that is, in the highly conductive state of the composite in which the films displayed simple, ohmic resistance behavior between two electrically conductive contacting leads. Such composites consist of highly interconnected networks of conductive particles in a matrix of insulating organic material, but the structure of the organic material is difficult to elucidate directly from scanning electron microscopy, X-ray photoelectron spectroscopy, or other spectroscopic methods because of the high mole fraction of carbon black in the composites.

Table 1a and Scheme 1 present information on the high (75%) and low (20−25%) carbon black loaded sensor arrays. The first exposure in Figure 1 shows the baseline-corrected resistance response of a nonpolymer− and polymer−carbon black composite sensor on exposure to *n*-hexane at $P/P^0 = 0.0050$. Shown are tetracosanoic acid/dioctyl phthalate (75% carbon black; sensor A4) and poly(ethylene-*co*-vinyl acetate) (40% carbon black; sensor C2) films, which both exhibited the highest signal and lowest noise for each of their respective sensor array types investigated. The resistance of all films increased when analyte vapor was present and rapidly (i.e., within seconds) returned to its original baseline resistance

Table 2. Sensor Response, $\Delta R/R_b$ ($\times$10 000), of (a) Carbon Black−Nonpolymer Composite Sensors (75% Carbon Black, Table 1a) and (b) Carbon Black-Polymer Composite Sensors to Seven Test Analytes Presented at a Concentration of $P/P^0 = 0.0050$[a]

sensor	*n*-hexane	ethanol	ethyl acetate	cyclohexane	*n*-heptane	*n*-octane	isooctane
			(a) Carbon Black−Nonpolymer Composite Sensors				
A1	4.2 ± 0.9	6.4 ± 0.8	8.0 ± 0.7	1.7 ± 0.3	4.4 ± 1.0	6.3 ± 1.0	3.1 ± 1.3
A2	−12.5 ± 7.2	15.0 ± 2.9	2.6 ± −5.1	−5.1 ± 2.9	−14.7 ± 9.3	−16.6 ± 9.4	−21.3 ± 10.8
A3	21.7 ± 2.9	1.3 ± 0.2	8.3 ± 0.8	8.9 ± 0.7	25.1 ± 4.5	38.0 ± 7.4	27.4 ± 4.1
A4	11.9 ± 2.1	1.0 ± 0.2	4.5 ± 0.7	5.6 ± 1.6	13.2 ± 3.8	19.9 ± 6.1	15.9 ± 4.0
A5	18.0 ± 0.9	0.9 ± 0.3	6.1 ± 0.5	5.2 ± 0.5	23.2 ± 0.9	36.5 ± 1.4	24.2 ± 0.8
A6	2.4 ± 0.3	6.9 ± 1.0	2.4 ± 0.4	1.6 ± 0.2	2.2 ± 0.4	2.7 ± 0.5	2.7 ± 0.4
A7	18.7 ± 1.0	0.8 ± 0.2	5.8 ± 0.3	6.8 ± 1.0	23.1 ± 1.5	35.6 ± 2.6	24.8 ± 1.2
			(b) Carbon Black-Polymer Composite Sensors				
C1	3.2 ± 0.2	6.1 ± 0.2	13.3 ± 0.3	4.9 ± 0.2	2.8 ± 0.2	2.8 ± 0.1	3.3 ± 0.1
C2	18.2 ± 0.5	12.0 ± 0.5	48.4 ± 1.3	27.9 ± 0.6	16.6 ± 0.5	17.9 ± 0.4	19.7 ± 0.5
C3	4.2 ± 0.4	3.2 ± 0.4	5.8 ± 0.2	5.6 ± 0.2	4.2 ± 0.2	4.7 ± 0.2	5.2 ± 0.2
C4	2.1 ± 0.2	2.7 ± 0.2	12.3 ± 0.4	3.4 ± 0.2	1.7 ± 0.2	1.6 ± 0.2	1.8 ± 0.2
C5	20.2 ± 0.6	6.6 ± 0.3	37.8 ± 1.1	31.0 ± 1.0	18.5 ± 0.6	20.1 ± 0.5	22.4 ± 0.5
C6	18.7 ± 0.6	11.9 ± 0.5	49.6 ± 1.9	28.7 ± 1.1	16.9 ± 0.6	18.2 ± 0.5	20.0 ± 0.5
C7	14.7 ± 0.5	7.5 ± 0.3	55.3 ± 2.0	23.8 ± 0.9	12.9 ± 0.5	13.5 ± 0.4	14.5 ± 0.3
C8	0.6 ± 0.1	1.5 ± 0.1	5.7 ± 0.2	0.5 ± 0.1	0.5 ± 0.1	0.4 ± 0.1	0.2 ± 0.1
C9	6.8 ± 0.5	12.2 ± 0.5	34.6 ± 0.9	6.1 ± 0.4	5.7 ± 0.4	5.2 ± 0.3	2.3 ± 0.3

[a] The sensors were subjected to 200 exposures to each analyte selected from 1400 randomly ordered exposures to seven test analytes. Means and standard deviations are given for each sensor (mean ± standard deviation).

value after the vapor exposure had been discontinued. Nonpolymer−carbon black composite sensors consistently displayed SNRs and response magnitudes comparable to those obtained with the well-studied polymer−carbon black composite sensors evaluated in this work.

Figure 1 also displays the response of a representative sensor (tetracosanoic acid/dioctyl phthalate) to *n*-hexane. Sensor responses shown were at 0, 1, 35, 44, 62 and 72 h in a run of randomized exposures to the seven test analytes. As observed in Figure 1, in all cases, the sensor fully returned to the same response on exposure to *n*-hexane at $P/P^0 = 0.0050$, as well as returned to the same baseline resistance on exposure to laboratory air. This was the case for the majority of exposures (>95%); however, hysteresis did occur randomly in a small percentage of exposures. Therefore, sensor responses were baseline corrected, forcing sensor readings to fully return to their initial baseline resistance; this ensured that $\Delta R_{max}/R_b$ was due solely to the sensor/analyte interaction and not due to sensor drift.

Table 2 presents the sensitivities and standard deviations of the responses measured for the seven different carbon black composite sensor compositions exposed to the seven test analytes studied in this work at an activity of $P/P^0 = 0.0050$ in air. Sensitivities varied significantly across the analytes tested, and a given analyte produced different responses on different sensor films.

Different levels of variability were observed in the response of each of the sensors. Part of this variability in the response amplitude can be ascribed to sensor noise, which is inherent and unique to each of the sensors, as well as to variation in room temperature during the exposures. For example, a 1 °C change in room temperature produces a 4.5% change in the vapor pressure of *n*-hexane (the vapor pressures of *n*-hexane at 20 and 21 °C are 119.9 and 125.3 Torr, respectively).[41] Additionally, slight (though significant) drift was observed for several of the sensors, though this did not affect the ability to accurately model and predict based on sensor array response patterns.

SNRs were calculated for each sensor on exposure to each of the test analytes. Table 3a details the means and standard deviations of the SNRs for each carbon black−nonpolymer composite sensor on exposure to the various test analytes each presented 200 times in random order at $P/P^0 = 0.0050$. For comparison, Table 3b presents the SNRs of the carbon black−polymer composite sensors on exposure to these analytes at the same partial pressure of $P/P^0 = 0.0050$. The two sensor types exhibited similar SNR values, with different sensors performing better in different cases.

B. Concentration Dependence of Sensor Response. Figure 2a,b displays the responses of several typical carbon black−nonpolymer composites as a function of the vapor phase concentration of *n*-hexane and ethanol, respectively. For the relatively low analyte concentrations used in this study, the sensor responses were well-described by a linear dependence on P/P^0, indicating operation above the percolation threshold. This relationship has also been observed for carbon black−polymer composite sensors operating above the percolation threshold.[35]

Table 4a presents the limits of detection based on the $\Delta R_{max}/R_b$ versus concentration data presented in Figure 2. SNRs were calculated (eq 4) for each of the sensors on exposure to hexane and ethanol at various fractions of their vapor pressure ($0.0020 < P/P^0 < 0.0625$), and detection was taken to be the partial pressure at which SNR = 3. Limits of detection ranged from $P/P^0 = 0.002$ to $P/P^0 = 0.0075$, with most values near 0.0035 or 0.005. These thresholds were converted to parts per million for display. For comparison, Table 4b gives detection limits for several carbon black−polymer composites, exposed simultaneously with optimized carbon black−nonpolymer composite sensors to ensure a representative comparison. The limits of detection for the carbon black−polymer composite sensors are in accord with values reported previously.[42] The carbon black−nonpolymer

(41) Weast, R. C. *CRC Handbook of Chemistry and Physics*, 70th ed.; CRC Press: Boca Raton, FL, 1989/1990.

(42) Doleman, B. J.; Lewis, N. S. *Sens. Actuators, B* **2001**, 41.

Table 3. SNRs of (a) Carbon Black−Nonpolymer Composite Sensors (75% Carbon Black, Table 1a) and (b) Carbon Black−Polymer Composite Sensors (Table 1c) to Seven Test Analytes Presented at a Concentration of $P/P^0 = 0.0050$[a]

sensor	*n*-hexane	ethanol	ethyl acetate	cyclohexane	*n*-heptane	*n*-octane	isooctane
			(a) Carbon Black−Nonpolymer Composite Sensors				
A1	90 ± 62	142 ± 89	99 ± 49	45 ± 31	73 ± 41	65 ± 31	38 ± 32
A2	−136 ± 109	109 ± 65	25 ± 22	−52 ± 45	−151 ± 145	−97 ± 79	−230 ± 172
A3	152 ± 62	16 ± 7	81 ± 33	86 ± 33	150 ± 41	164 ± 36	155 ± 46
A4	100 ± 49	13 ± 6	46 ± 19	54 ± 30	97 ± 51	131 ± 44	101 ± 40
A5	55 ± 19	5 ± 4	25 ± 14	22 ± 15	64 ± 23	73 ± 18	75 ± 36
A6	25 ± 10	68 ± 34	24 ± 11	18 ± 8	23 ± 10	27 ± 10	29 ± 13
A7	99 ± 26	14 ± 8	61 ± 27	82 ± 38	98 ± 23	90 ± 17	112 ± 24
			(b) Carbon Black−Polymer Composite Sensors				
C1	102 ± 40	102 ± 40	505 ± 190	215 ± 81	134 ± 54	138 ± 46	143 ± 58
C2	465 ± 211	211 ± 102	763 ± 187	809 ± 276	586 ± 220	636 ± 240	746 ± 313
C3	32 ± 12	30 ± 10	107 ± 45	61 ± 22	39 ± 14	43 ± 16	56 ± 23
C4	29 ± 12	62 ± 23	190 ± 87	60 ± 22	32 ± 11	35 ± 14	42 ± 20
C5	104 ± 45	53 ± 21	193 ± 76	182 ± 75	133 ± 51	146 ± 56	198 ± 84
C6	46 ± 21	311 ± 124	585 ± 278	68 ± 32	54 ± 20	46 ± 18	38 ± 15
C7	238 ± 77	146 ± 57	1355 ± 654	526 ± 217	295 ± 181	304 ± 111	320 ± 123
C8	30 ± 12	87 ± 38	206 ± 80	24 ± 8	34 ± 15	33 ± 13	15 ± 8
C9	65 ± 30	54 ± 23	326 ± 111	49 ± 13	77 ± 32	70 ± 22	29 ± 11

[a] The sensors were subjected to 200 randomly ordered exposures to each of the seven test analytes. Means and standard deviations are given for each sensor (mean ± standard deviation).

Table 4. Approximate Limits of Detection in PPM of (a) Carbon Black−Nonpolymer Composite Sensors (Table 1a) and (b) Carbon Black−Polymer Composite Sensors (Table 1c) for the Detection of *n*-Hexane and Ethanol[a]

(a) Carbon Black−Nonpolymer Composite Sensors

	sensor						
analyte	A1	A2	A3	A4	A5	A6	A7
n-hexane	110	100	100	100	100	60	140
ethanol	50	50	50	40	40	40	40

(b) Carbon Black−Polymer Composite Sensors

	sensor			
analyte	PVS (C8)	PEVA (C2)	PCL (C1)	PEO (C3)
n-hexane	120	140	160	140
ethanol	70	50	80	50

[a] The limit of detection is defined as the vapor concentration in PPM at which SNR = 3.

composite sensors exhibited comparable detection limits when compared to these well-studied and developed carbon black−polymer composite sensors.

C. Sensor Specificity. Figure 3 presents the mean responses, averaged over 200 randomly ordered exposures to each analyte, for each of the carbon black−nonpolymer composite films to the seven test analyte vapors at $P/P^0 = 0.0050$. Large differences in sensitivity were observed between the responses of a given sensor upon exposure to the various test analytes. For example, quinacrine dihydrochloride dihydrate (sensor A2) displayed a strong positive response on exposure to a prototypical polar analyte, ethanol, while displaying a strong negative response to a prototypical nonpolar analyte, *n*-hexane. This can be attributed to insolubility of the latter compound with nonpolar solvents resulting from dielectric constant differences and molecular size. Additionally, a tetracosanoic acid/dioctyl phthalate−carbon black composite (sensor A7) exhibited an *n*-hexane/ethanol response ratio of 22, while a quinacrine dihydrochloride dihydrate/dioctyl phthalate−carbon black composite (sensor A6) displayed an *n*-hexane/ethanol response ratio of 0.3. For comparison, of the polymer−carbon black composite sensors investigated, the greatest response ratio of ethanol to *n*-hexane was produced by poly(ethylene-*co*-vinyl acetate) (sensor C2), with a ratio of 4, and the smallest ratio was achieved by poly(vinyl butyral) (sensor C8), with a ratio of 0.4 (Table 2b). Clearly, the use of organic molecular sorption phases having a high density of hydrophilic or hydrophobic functional groups can produce sensor arrays that display large discrimination power between differing test pairs of analytes.

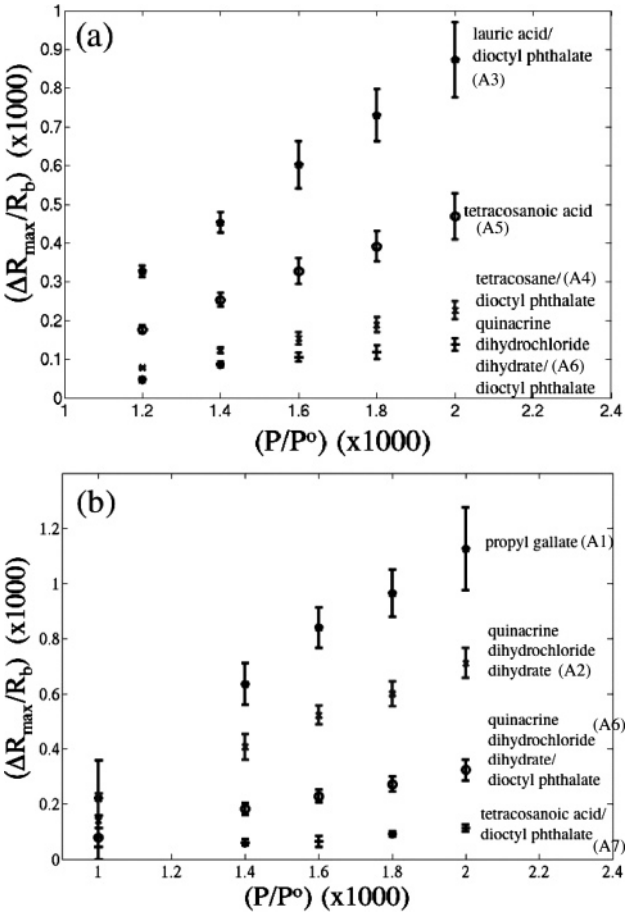

Figure 2. Plot of several nonpolymer−carbon black composite sensor responses (75% carbon black), $\Delta R_{max}/R_b$, to (a) *n*-hexane and (b) ethanol at various concentrations.

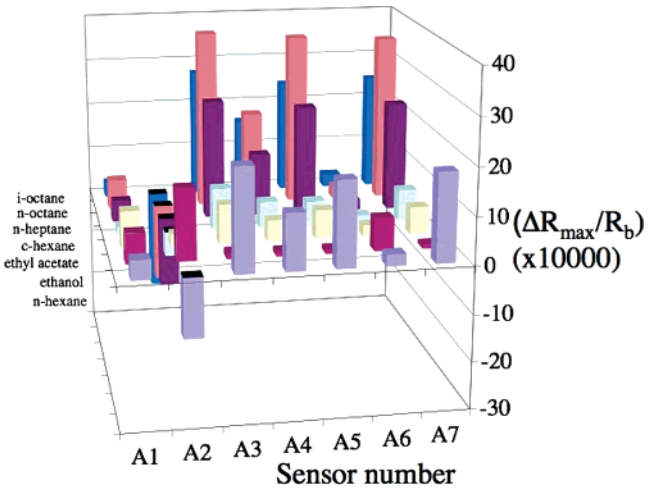

Figure 3. Three-dimensional pattern depicting the average carbon black−nonpolymer sensor responses (Table 1a) to the seven test analytes at a concentration of $P/P^0 = 0.0050$ in air. Standard deviations of the sensor responses are given in Table 2a.

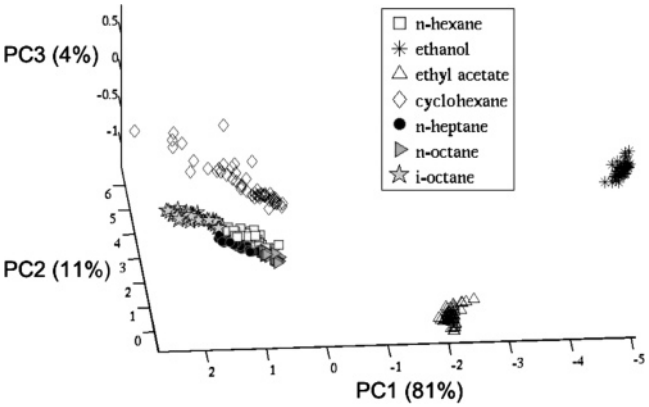

Figure 4. Principal components analysis showing principal components 1, 2, and 3 from normalized sensor array response data. For visualization ease, only the first 50 exposures to each of the test analytes are analyzed are shown. The valves in parenthesis are the percentage of the total variance in each principal component.

D. Sensor Array Response to Various Analytes. Principal components analysis[27] was used to visualize the differences in normalized autoscaled response patterns of a seven element carbon black composite sensor array (Table 1a) exposed randomly 200 times to each of the seven test analytes at $P/P^0 = 0.0050$. The points plotted in Figure 4 represent unique response patterns of the sensor array to each of the analytes presented. The response vectors are displayed with respect to the first three principal components of the data set, which contained 96% of the variance in detector response. Several major clusters are observed: ethanol, ethyl acetate, and cyclohexane, as well as a clustering of the remaining alkanes. This remaining cluster of alkanes also displays a distinct pattern, which can also be seen in Figure 4. Even at the relatively low analyte concentrations used in this study, the sensor array readily distinguished extremely well between polar and nonpolar analytes, as well as providing reasonable clustering among very similar polar analytes.

The classification performance of the sensor array was quantified by use of the FLD algorithm for pairwise analyte classification. The figure of merit to determine the effectiveness of the FLD model is the resolution factor, rf (eq 3), which quantifies the statistical separation between the two data clusters of interest. The first 100 normalized exposures to each analyte were used as a training set, and the remaining 100 normalized exposures to each analyte, from the same set of data collection, were used as a test set. This train/test scheme was adopted to avoid bias resulting from possible overfitting of data.

Table 5. Resolution Factors Displaying the Ability of the (a) Carbon Black−Nonpolymer Composite Sensor Array (Table 1a, Sensors A1−A7) and (b) Carbon Black−Polymer Composite Sensor Array (Table 1c, Sensors C1−C9; from Raw Data Previously Reported[43]) To Distinguish between Test Analytes Presented at $P/P^0 = 0.0050$[a]

analyte	*n*-hexane	ethanol	ethyl acetate	cyclo-hexane	*n*-heptane	*n*-octane	iso-octane
(a) Carbon Black−Nonpolymer Composite Sensor Array							
n-hexane	N/A	44.6	13.3	6.1	6.4	9.9	6.2
ethanol		N/A	27	36.5	47.5	51.7	50
ethyl acetate			N/A	14.3	15.4	20.6	14.5
cyclohexane				N/A	8.2	10.1	6.9
n-heptane					N/A	4.2	3.7
n-octane						N/A	4.8
isooctane							N/A
(b) Carbon Black−Polymer Composite Sensor Array							
n-hexane	N/A	10.73	6.13	2.47	1.23	1.65	3.49
ethanol		N/A	24.2	29.1	23.28	25.23	25.85
ethyl acetate			N/A	30.42	15.51	27.09	32.09
cyclohexane				N/A	3.94	4.43	10.23
n-heptane					N/A	1.67	6.81
n-octane						N/A	6.73
isooctane							N/A

[a] In each case, for a given separation task, a FLD model was trained on exposures 1−100, and exposures 101−200 were then tested using the model. Reported values are for exposures 101−200.

Table 5a presents resolution factors for the carbon black−nonpolymer composite sensor array (sensors A1−A7). For comparison, Table 5b presents resolution factors for an array of carbon black−polymer composite sensors consisting of the nine polymers (sensors C1−C9) given in Table 1c. This nine-sensor carbon black−polymer composite array was chosen from a nonexhaustive search seeking the best nine-sensor array that maximized the resolution factors for the worst-resolved pairs (>15 nine-sensor array combinations were investigated, and the "best" sensors based on experience, polycaprolactone, poly(ethylene-*co*-vinyl acetate), and poly(ethylene oxide), were always included). In terms of the ability to resolve various analytes, the nonpolymeric composite sensor array performed highly favorably relative to the well-developed and well-studied polymer-based sensor array, with significant increases in resolution in many previously difficult classification tasks. For example, in classifying *n*-hexane from cyclohexane, *n*-heptane, *n*-octane, or isooctane, resolution factors of 2.5, 1.2, 1.7, and 3.5, respectively, were observed for the polymer composite-based sensor array. The use of a carbon black−nonpolymer composite sensor array increased these resolution factors to 6.1, 6.4, 9.9, and 6.2, respectively. A resolution factor of 1 implies 68% correct classification, 2 implies 95.5% correct classification, and 3 implies 99.7% correct classification. This new sensor type thus takes previous classification tasks which perform at levels slightly above chance, and provides the ability to consistently and confidently correctly classify such analytes.

E. Stability and Drift. A FLD model for each binary separation task, consisting of projection weights and a

Table 6. Performance Values of a Low Mass Fraction Carbon Black−Nonpolymer Composite Sensor Array (Table 1b, Sensors B1−B9) in Various Binary Separation Tasks[a]

analyte	*n*-hexane	ethanol	ethyl acetate	cyclo-hexane	*n*-heptane	*n*-octane	iso-octane
			(a) Data Set 1				
n-hexane	N/A	1	1	1	0.82	0.95	1
ethanol		N/A	1	1	1	1	1
ethyl acetate			N/A	1	1	1	1
cyclohexane				N/A	1	1	0.92
n-heptane					N/A	0.84	1
n-octane						N/A	1
isooctane							N/A
			(b) Data Set 2				
n-hexane	N/A	1	1	1	0.73	0.79	1
ethanol		N/A	1	1	1	1	1
ethyl acetate			N/A	1	1	1	1
cyclohexane				N/A	1	1	0.56
n-heptane					N/A	0.59	1
n-octane						N/A	1
isooctane							N/A
			(c) Data Set 3				
n-hexane	N/A	1	1	0.99	0.66	0.79	1
ethanol		N/A	1	1	1	1	1
ethyl acetate			N/A	1	1	0.99	1
cyclohexane				N/A	0.99	0.99	0.54
n-heptane					N/A	0.64	1
n-octane						N/A	1
isooctane							N/A
			(d) Data Set 4				
n-hexane	N/A	0.94	0.98	0.51	0.51	0.5	0.59
ethanol		N/A	1	0.88	0.95	0.91	0.98
ethyl acetate			N/A	0.99	0.98	0.99	0.9
cyclohexane				N/A	0.52	0.51	0.5
n-heptane					N/A	0.5	0.59
n-octane						N/A	0.62
isooctane							N/A

[a] Trained on the first 100 exposures to (a) data set 1 and applied to various sets of data collection, with various times between each set of data collection. (b) Data set 2, (c) data set 3, and (d) data set 4 were collected 2 days, 6 days, and 6 months, respectively, after the initial data set that trained the Fisher model used for classification.

decision boundary, was constructed from sensor responses in the first data set of the first 100 exposures to each analyte. This model was then applied to 700 subsequent exposures spread over four sets that spanned six months of data collection. The exposures for each binary separation task were then projected onto the FLD vector characteristic for the given separation task, placing data into the one-dimensional space which initially maximized the resolution factor between the two analytes of interest. These analyte projections were compared to the originally modeled decision boundary for the given binary separation and thereby assigned to be in one of the two analyte clusters. The performance factor is defined as the number of correct classifications divided by the number of classification attempts. Table 6 lists the performance factors for all combinations of binary separations for each set of data collection.

Binary separation performances were comparable throughout the first three data sets, which spanned 1 month. However, the fourth data set, collected 6 months after the initially trained model, yielded extremely low classification performance in many situations. In terms of the Fisher model, two possible explanations of this performance loss are (1) that a new dimension for each binary analyte separation captures maximum resolution between analyte clusters, so that a new model, with different projection weights for each analyte, and a new decision boundary need to be created, or (2) that the same model approximately captures maximum resolution between analyte clusters, but the clusters have drifted with respect to the original decision boundary. In the latter case, a calibration scheme has proven capable of restoring the classification performance of carbon black−polymeric composite sensors.[43] To compensate for this type of drift, sensor responses were adjusted by a multiplicative calibration factor:

$$S_{a,t} = S_{c,t}\frac{S_{a,0}}{S_{c,0}} \tag{5}$$

where $S_{a,t}$ and $S_{c,t}$ indicate the $\Delta R/R_b$ response signals for an analyte a and calibrant c, respectively, at some time t after training, and $S_{a,0}$ and $S_{c,0}$ are the initial responses to analyte a and calibrant c.[43]

Table 7 presents the classification performance for each binary separation, using each analyte as a calibrant, when the initial model (based on exposures 1−100, data set 1) was used on the final data set (200 exposures, recorded 6 months after the initial data set). The first three exposures from the final data set were used to calibrate the model according to eq 5 and were then followed by 47 test exposures. This cycle of calibrate/test was repeated three additional times, accounting for all 200 exposures of the final data set. For clarity, performances are given for binary separations both without the use of calibration and for the calibrant that proved most effective; cases where reasonable performances are attained are shown in bold text. Of the 21 combinations of binary analyte separations, 17 yielded performance scores of ≥ 0.90.

For binary separations with low performance values, even after the calibration scheme was employed, the sensor array was still capable of resolving between analyte pairs in the data set; however, a rigorous training period was again required to construct a new model for effective analyte separation. For example, the binary classification of *n*-hexane and *n*-heptane yielded a performance of 0.49 and had a resolution factor of 0.02 when the initial model was applied to the final data set. However, if the first 100 exposures of data set 4 were used to construct a new model, a resolution factor of 1.5 and a classification performance of 0.88 were achieved for the final 100 exposures of data set 4. These values are comparable to those obtained from training on the first 100 exposures and testing on the final 100 exposures of data set 1, with a resolution factor and performance of 1.5 and 0.88, respectively (Tables 5 and 6). Thus, no sensor performance was lost, but the initial model describing the sensor response behavior changed significantly, resulting in the loss of predictive ability.

Figure 5a shows projections of 700 exposures, spread over four sets of data collection, for a FLD model constructed from the first 100 exposures in data set 1. Figure 5b shows these same projections, when a calibration scheme was adopted in which three exposures were first used as calibrant runs, followed by 47 test exposures, with the process repeated

(43) Sisk, B. C.; Lewis, N. S. *Sens. Actuators, B* **2005**, *104*, 249.

Table 7. Performance Values of Carbon Black−Nonpolymer Composite Sensors (B1−B9) when a FLD Model Was Trained on 100 Exposures and Tested on 200 Exposures 6 Months Later, with the Use of Calibration[a]

	calibrant used							calibrant comparison	
classification task	*n*-hexane	ethanol	ethyl acetate	cyclohexane	*n*-heptane	*n*-octane	isooctane	no calibrant	best calibrant
***n*-hexane/ethanol**	0.58	0.98	1	0.82	0.86	0.96	0.95	**0.94**	**1**
***n*-hexane/ethyl acetate**	0.57	0.96	0.98	0.7	0.85	0.73	0.84	**0.98**	**0.98**
***n*-hexane/cyclohexane**	0.86	0.52	0.51	0.83	0.88	0.9	0.74	**0.51**	**0.9**
n-hexane/*n*-heptane	0.5	0.56	0.55	0.5	0.53	0.5	0.49	0.51	0.56
n-hexane/*n*-octane	0.49	0.57	0.56	0.51	0.53	0.55	0.51	0.5	0.57
***n*-hexane/isooctane**	0.91	0.59	0.6	0.88	0.95	0.97	0.86	**0.59**	**0.97**
ethanol/ethyl acetate	0.51	1	1	0.75	0.84	0.86	0.76	**1**	**1**
ethanol/cyclohexane	0.58	0.95	0.99	0.83	0.85	0.98	0.95	**0.88**	**0.99**
ethanol/*n*-heptane	0.59	0.9	0.99	0.83	0.86	0.98	0.97	**0.95**	**0.99**
ethanol/*n*-octane	0.57	0.89	0.99	0.84	0.85	0.97	0.96	**0.91**	**0.99**
ethanol/isooctane	0.57	0.99	1	0.85	0.86	0.99	0.98	**0.98**	**1**
ethyl acetate/cyclohexane	0.57	0.86	0.98	0.73	0.84	0.73	0.83	**0.99**	**0.98**
ethyl acetate/*n*-heptane	0.58	0.76	0.97	0.71	0.85	0.74	0.85	**0.98**	**0.97**
ethyl acetate/*n*-octane	0.57	0.97	0.99	0.72	0.85	0.74	0.85	**0.99**	**0.99**
ethyl acetate/isooctane	0.53	0.53	0.89	0.72	0.81	0.72	0.82	**0.9**	**0.89**
cyclohexane/*n*-heptane	0.86	0.7	0.68	0.82	0.86	0.91	0.78	**0.52**	**0.91**
cyclohexane/*n*-octane	0.9	0.91	0.79	0.82	0.91	0.95	0.83	**0.51**	**0.95**
cyclohexane/isooctane	0.48	0.5	0.5	0.58	0.48	0.54	0.57	0.5	0.58
n-heptane/*n*-octane	0.49	0.52	0.51	0.5	0.51	0.54	0.51	0.5	0.54
***n*-heptane/isooctane**	0.89	0.89	0.8	0.88	0.93	0.97	0.9	**0.59**	**0.97**
***n*-octane/isooctane**	0.89	0.9	0.88	0.87	0.91	0.96	0.91	**0.62**	**0.96**

[a] Scenarios for the best calibrant and for the use of no calibrant are listed for direct comparison; binary separation tasks capable of high performances with a 6 month period between the training and the test phases are shown in bold.

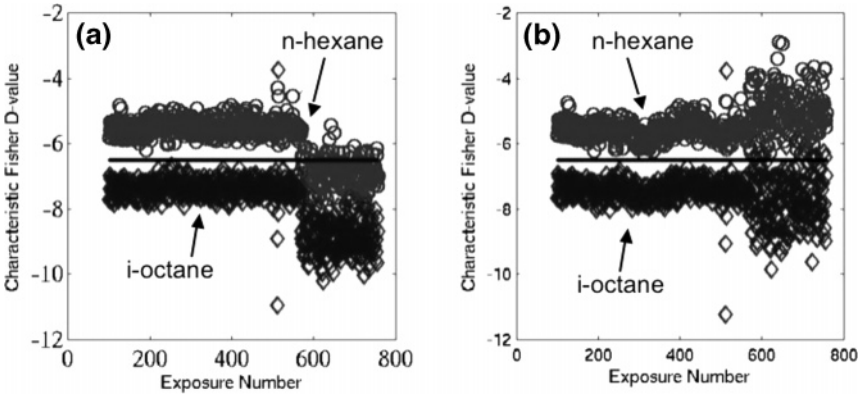

Figure 5. "Waterfall" plots detailing drift of *D* values (the single dimensional projection of the sensor array response which initially maximized the resolution factor for the classification task at hand) vs exposure number for the *n*-hexane/isooctane binary separation task. The first 100 exposures of data were used to train the model. A decision boundary (solid line) based on these first 100 exposures is shown. Results are shown for (a) no calibration and for (b) calibration using *n*-octane.

throughout the remaining 700 exposures of the data set. The projected dimension clearly maintained a reasonable level of separation between the two analytes (although this is no longer the optimal one-dimensional space for resolution); however, the analyte clusters drifted relative to the decision boundary. The calibration process shifted these projections back to the decision boundary, and classification performance was restored.

IV. Discussion

The vapor sensing properties of the carbon black−nonpolymeric composite sensors and sensor arrays compare favorably in all aspects to the well-investigated carbon black−polymer composite sensing films. The nonpolymeric sensors provide improved analyte clustering and greater analyte resolution/classification capability, as well as a high level of signal-to-noise and low detection limit thresholds.

A measure of the performance of a sensor array is the resolution factor, which is a measure of the ability of a given sensor array to distinguish between and discriminate among various analytes. In this respect, the carbon black−nonpolymer composite sensors surpass the performance of previous sensor classes, including the well-studied carbon black−polymer composite sensors (Table 5a,b). Significant improvements were observed, in particular, in the ability of the sensor array to distinguish between various types of alkanes, namely, *n*-hexane, cyclohexane, *n*-heptane, *n*-octane, and isooctane.

The nonpolymeric sensors are well-suited to detect and exploit subtle differences between analytes, owing to a higher density and random arrangement of functional groups, as well as an enhanced SNR for analyte detection. In typical carbon black−polymer composite sensors, functional groups are present at certain repeat units along the polymer backbone, and this structural motif places a limit on the functional group density as well as a limit on possible analyte−polymer interactions, due to steric hindrance. With the carbon black−nonpolymer composite sensor array, a higher functional group density, as well as random packing, can provide more specific sensor−analyte interactions which are able to better

capture subtle differences in analyte properties. High SNRs provide the means of detecting and describing these subtle differences, which would likely be lost in the noise of other sensor types. These combinations allow carbon black−nonpolymer composite sensors to more precisely define the position of extremely similar analytes in sensor space, which translates into enhanced clustering and resolution ability.

The carbon black−nonpolymer composite sensors also exhibited lower detection limits relative to typical carbon black−polymer composite sensors (Table 4a,b). Thus, carbon black−nonpolymer composite sensors are more suitable for trace vapor detection, which broadens the potential areas of application of these sensors.

The low mass fraction carbon black−nonpolymer sensor array showed relatively little long-term drift over extended time periods. Specifically, for most binary separation tasks, the nonpolymeric composite sensors provided good analyte classification levels for at least 6 months after an initial training phase. When the sensors were used 6 months after an initial training period, 11 of the 21 binary separation tasks were performed with correct classification rates of >90% (Tables 6 and 7). When a simple calibration scheme, which involved only 3 calibration exposures per 50 exposures, was performed, the number of binary separation tasks with >90% correct classification after six months increased to 17. Those cases where performance was unacceptable even after calibration are the same as those reported for carbon black−polymer composite sensors, for example, *n*-hexane versus *n*-heptane or *n*-heptane versus *n*-octane.[43]

Plasticizers such as dioctyl phthalate (a viscous liquid) have been added to polymers to lower their glass transition temperature and decrease the sensor response time to various vapors. The sensors studied herein showed response times that were rapid, both with and without the presence of dioctyl phthalate or similar plasticizers (Figure 1). This rapid time response is characteristic of the use of low molecular weight nonpolymeric organic molecules as the sorbent phase.

For many diseases, specific volatile organic compounds such as amines and fatty acids are found in the breath and urine of infected individuals. For bio-sensing applications, it is desirable to have sensors with a high sensitivity to these species. A key feature of using molecularly based sorbent phases is the ability to tune the sensitivity toward different classes of chemicals. The ratios of the $\Delta R_{max}/R_b$ responses of two carbon black−nonpolymer composite sensors, tetracosanoic acid/dioctyl phthalate and quinacrine dihydrochloride dihydrate/dioctyl phthalate, on exposure to *n*-hexane and to ethanol, were 22 and 0.3, respectively. Additionally, the sensor consisting of pure quinacrine dihydrochloride dihydrate exhibited a strong positive response on exposure to polar analytes and a strong negative response on exposure to nonpolar analytes. Such large differences for various other analytes could likely be produced by further development of this class of sensors.

V. Conclusions

Composites made from homogeneous or blended organic molecules and carbon black showed fast response times, good reversibility, high stability, and an excellent ability to discriminate and classify between both similar and dissimilar types of analytes. This type of composite sensor offers a higher density of functional groups, as well as a random orientation and random exposure of these functional groups within the sensing material due to the lack of a restricting polymer backbone. A seven-sensor array robustly resolved even extremely similar test analytes, such as *n*-hexane and *n*-heptane. Excellent SNRs can be achieved with these carbon black−nonpolymer composite sensors, which provide comparable limits of detection relative to the evaluated carbon black−polymer composite sensors.

Acknowledgment. The authors thank Dr. Brian Sisk, Dr. Erik J. Severin, and Edgardo García-Berríos for valuable discussions. Research was carried out in the Molecular Materials Research Center of the Beckman Institute at Caltech. This work was partially supported by the National Institutes of Health and by the ARO under the Institute for Collaborative Biotechnologies.

CM060905X